JEAS

Analysis of the Effects of Pipe Specifications on the Critical Flow Velocity of Fluid

Okonkwo Ugochukwu C, Egu Gregory Ibe Onyenobi and Samuel Chinwendu
Department of Mechanical Engineering, Nnamdi Azikiwe University Awka, Anambra State, Nigeria
*Corresponding Author's E-mail: greg_egu@yahoo.com

Abstract

This study applied the finite element method to analyse the internal flow induced vibration in a pinned-pinned pipe, while studying the effects of increasing the length of the pipe span and the pipe bore diameter, on the critical flow velocity. The pipe is undamped, and of rigid polyvinylchloride material. However, the fluid-pipe system experiences a gyroscopic damping arising from Coriolis force. The analysis was carried out on pipe span lengths of 2m, 3m, 4m, 5m, and 6m, with corresponding 20, 24, 30, 42, and 50 elements respectively. Further analysed was the 2m pipe span length with the following respective bore diameters: 0.0389m, 0.0570m, 0.0697m, 0.0856m, 0.111m. All pipes maintained a uniform thickness of 0.00165m. The fluid is water, an incompressible, non-volatile fluid, flowing at room temperature. The results are shown by graphical plots. For the 2m, 3m, 4m, 5m, and 6m pipes span lengths, the values of critical velocity obtained were 17.80 m/s , 10.00 m/s, 7.80 m/s, 6.20 m/s, and 5.90 m/s respectively, while 2m length pipes of bore diameters, 0.0389m, 0.0570m, 0.0697m, 0.0856m, and 0.111m each, produced the following respective values of critical velocity, 17.80 m/s, 20.50 m/s, 22.50 m/s, 24.70 m/s, and 27.89 m/s. Generally, the finite element method showed that critical velocity reduces with increasing pipe span length and increases with increasing pipe bore diameter.

Keywords: Finite Element Method, Pinned-Pinned Pipe, Critical Velocity, Pipe Span Length, Pipe Bore Diameter.

1. Introduction

Vibration problems due to fluid flow occur in many industrial applications. Internal flow induced vibration in pipes can occur due to high velocity steady flow speeding up to the critical velocity or due to the presence of unsteady flow such as pulsating turbulent flow in the piping, thereby generating vibration excitation forces. The study of these phenomena draws on three disciplines: structural mechanics, mechanical vibration and fluid dynamics. The dynamic behaviour of fluid conveying pipes are more complicated than their non-fluid conveying counterparts owing to internal forces developed from fluid-structure interaction in the former. In the course of its flow, the flowing fluid imposes pressure on the walls of the pipe which impacts stresses on the pipe material. (Ubani et al. 2013). The resultant vibration of the pipe produced by lateral momentum of flowing fluid pushes the pipe to a point of instability beyond which it may fail. Durrani (2001) developed a finite element methodology for the application of Coriolis force on a fluid filled pipeline. He presented nine case studies using finite element method and actual industrial project data. The data from his results showed noticeable gyroscopic damping effects of Coriolis force at relatively higher flow velocities.

Paıdoussis et al. (2002) studied the linear dynamics as well as the non-linear dynamics of cylindrical cantilever pipes conveying axially flowing fluid. They identified flow velocity increase, as the primary reason for the divergent form of loss of stability in the pipe. Using the homotopy perturbation method, Xu et al. (2010) proposed an analytical expression of natural frequencies of fluid conveying pipes. They showed that the natural frequency of vibration reduces with increase in fluid velocity for the first three modes of the pinned-pinned pipe. Ojetola et al. (2011) while considering the effects of fluid mass and coriolis acceleration reported an analytical solution for the determination of natural frequencies, mode shapes, modal loss factors and stability conditions of the pipe. Ali et al. (2013) analysed the free vibration of pipes transporting fluid while resting on an elastic support. They calculated three eigen values of the Timoshenko beam for various values of stiffness and found that natural frequency parameter was

decreased with increasing values of mass ratio. Dagh and Sinir (2015) modelled the dynamical behaviour of the pipes using Euler-Bernoulli theory and found that the value of natural frequencies was higher under tensile effect due to the immovable end conditioned. Kokare and Paward (2015) in their study of velocity and pressure distributions in fluid flow found that natural frequencies of pipe decreases with increasing thickness of cantilever pipe and increases with thickness of clamped pipes. Chellapilla et al. (2016) investigated the weld tension effect on the flexural frequencies of guided pipes with a simple support, and concluded that the pipe was more stable at at lower fluid velocity and steady state conditions. Wen et al. (2016) considered the effect of pipe wall thickness, fluid pressure and fluid velocity while studying the fluid structure interaction (FSI) behaviour of pipelines, and presented several pipeline schemes illustrating the application of the proposed method. Jweeg and Ntayeesh (2016) developed a new approach using experiment, for estimating the buckling critical velocities in pipes conveying fluid, for increase in fluid pressure and have found fluid pressure to reduce critical velocity, as it increases, for clamped-pinned, pinned-pinned, and clamped-clamped pipes.

From literature, several portions of pipe and fluid parameters, and imposed conditions have been studied. The objective of this paper is to apply finite element modelling in the study of the effect of increasing the pipe span length and the pipe bore diameter on the critical velocity of fluid flow in a simply supported pipe. Possibly, a higher value of critical velocity may be attained by either or both of these pipe geometry modifications, to the end that the pipe may remain stable at higher flow velocities than its initial critical velocity.

2.0 Material and methods
The fluid conveying pipe is considered to be a uniform pipe of:
Length L, Internal perimeter S, transverse moment of inertia I, and internal cross sectional area A, conveying fluid of mass per unit length $M = \rho A$ with a mean axial flow velocity U.
The equation of motion governing the vibration of the fluid-pipe system is:

$$\frac{EI\,\partial^4 Y}{\partial x^4} + \frac{\rho A U^2 \partial^2 Y}{\partial x^2} + \frac{2\rho A U \partial^2 Y}{\partial x dt} + \frac{(\rho A + m)\partial^2 Y}{\partial t^2} = 0 \tag{1}$$

Where
ρA = Fluid Mass per unit length (fluid density x internal cross sectional area)
and
m = Mass of pipe per unit length

$\frac{EI\,\partial^4 Y}{\partial x^4}$ is the stiffness term, a force acting on the pipe due to its bending.

$\frac{\rho A U^2 \partial^2 Y}{\partial x^2}$ is the curvature term, a force acting on the pipe and conforming the flow of fluid to its curvature in bend.

$\frac{2\rho A U \partial^2 Y}{\partial x dt}$ is the coriolis force term, a force required to rotate the fluid element as each point in the pipe span rotates with an angular velocity .

$\frac{(\rho A + m)\partial^2 Y}{\partial t^2}$ is the inertia force term, a force acting on the pipe due to the inertia of the pipe and the fluid flowing through it.

2.1 Finite Element Modelling
The finite element procedure is given as follows:
1. Selection/Choice of Element.
2. Discretization of the domain into finite sub domains (elements).
3. Selection of interpolation function (the value of field variables at specific points referred to as nodes).
4. Development of the element matrix for the sub domains (elements).
5. Matrix Assembly of the element matrices of each sub domain to obtain the global matrix for the entire domain.
6. Application of the boundary conditions.
7. Solution of equations.
8. Display of results.

2.1.1 Selection/Choice of Element Type

The Euler-Bernoulli beam element with four degrees of freedom, two displacement (w) and two rotational (θ)respectively as shown in Figure 1, is chosen.
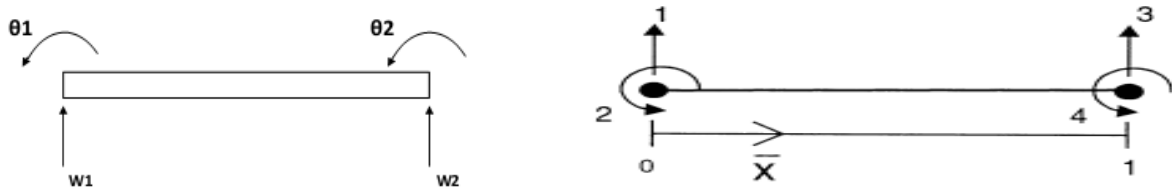
Grant (2010)

Figure 1: Euler-Bernoulli beam elements illustrating displacement and rotational degrees of freedom

2.1.2 Discretization

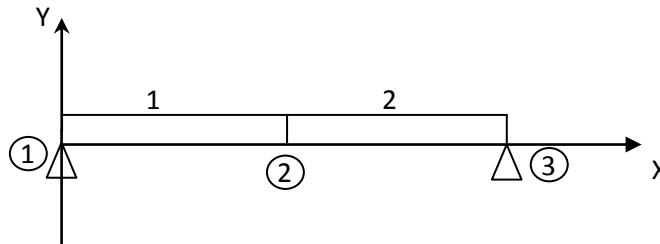The pipe is discretized into finite beam elements connected by nodes as shown

Figure 2: A Discretized Beam Model with Two Elements and Three Nodes

2.1.3 Selection of interpolation functions (Shape Functions)

The lateral displacement can be expressed in terms of shape functions as:

$$Y(x,t) = W(x,t) = [N(x)]\{W(t)\}_e \tag{2}$$

$N(x)$is the shape function identical to N_w and $\{W(t)\}_e$ is the nodal displacement at the node points.

The shape functions are given by:

$$N_1 = 1 - 3\left(\frac{x}{l}\right)^2 + 2\left(\frac{x}{l}\right)^3 \tag{3}$$

$$N_2 = x[1 - 2\left(\frac{x}{l}\right) + \left(\frac{x}{l}\right)^2] \tag{4}$$

$$N_3 = 3\left(\frac{x}{l}\right)^2 - 2\left(\frac{x}{l}\right)^3 \tag{5}$$

$$N_4 = x[-\left(\frac{x}{l}\right) + \left(\frac{x}{l}\right)^2] \tag{6}$$

2.1.4 Development of Element Matrices

Integrating over the entire length of the pipe (L)

$$\left\{\int_0^L \frac{EI\,\partial^4 Y}{\partial x^4} + \int_0^L \rho A U^2 \frac{\partial^2 Y}{\partial x^2} + \int_0^L 2\rho A U \frac{\partial^2 Y}{\partial x \partial t} + \int_0^L (\rho A + m)\frac{\partial^2 Y}{\partial t^2}\right\} dx = 0 \tag{7}$$

Rewriting 7 in terms of $W(x,t)$ (recall that $Y(x,t) = W(x,t)$ from 2) we have:

$$\left\{\int_0^L \frac{EI\,\partial^4 W(x,t)}{\partial x^4} + \int_0^L \rho AU^2 \frac{\partial^2 W(x,t)}{\partial x^2} + \int_0^L 2\rho AU \frac{\partial^2 W(x,t)}{\partial x \partial t} + \int_0^L (\rho A + m) \frac{\partial^2 W(x,t)}{\partial t^2}\right\} dx = 0 \qquad (8)$$

Substituting equation 2 into 7 we have:

$$\left\{\int_0^L \frac{EI\,\partial^4 [N(x)]\{W(t)\}}{\partial x^4} + \int_0^L \rho AU^2 \frac{\partial^2 [N(x)]\{W(t)\}}{\partial x^2} + \int_0^L 2\rho AU \frac{\partial^2 [N(x)]\{W(t)\}}{\partial x \partial t} + \int_0^L (\rho A + m) \frac{\partial^2 [N(x)]\{W(t)\}}{\partial t^2}\right\} dx = $$
$$0 \qquad (9)$$

The substitution and integration over the pipe length yields, in simple terms of N and W, the following equation

$$(\rho A + m)\,[S_1]\ddot{W} + 2\rho AU[S_3]\dot{W} + \{EI[S_2] + \rho AU^2[S_4]\}W = 0 \qquad (10)$$

Where

$$[S_1] = \int_0^L [N]^T[N]\,dx \qquad (11)$$

$$[S_2] = \int_0^L [N'']^T[N'']\,dx \qquad (12)$$

$$[S_3] = \int_0^L [N']^T[N]\,dx \qquad (13)$$

$$[S_4] = \int_0^L [N']^T[N']\,dx \qquad (14)$$

So that equation 10 expands to

$$\frac{(\rho A + m)l}{420}\begin{bmatrix} 156 & 22l & 54 & -13l \\ 22l & 4l^2 & 13l & -3l^2 \\ 54 & 13l & 156 & -22l \\ -13l & -3l^2 & -22l & 4l^2 \end{bmatrix}\begin{bmatrix} \ddot{W}_1 \\ \ddot{\theta}_1 \\ \ddot{W}_2 \\ \ddot{\theta}_2 \end{bmatrix} + \frac{\rho AU}{30}\begin{bmatrix} -30 & 6 & 30 & -6 \\ 6 & 0 & 6 & -1 \\ -30 & -6 & 30 & 6 \\ 6 & 1 & -6 & 0 \end{bmatrix}\begin{bmatrix} \dot{W}_1 \\ \dot{\theta}_1 \\ \dot{W}_2 \\ \dot{\theta}_2 \end{bmatrix}$$

$$+ \left\{\frac{EI}{l^3}\begin{bmatrix} 12 & 6l & -12 & 6l \\ 6l & 4l^2 & -6l & -2l^2 \\ -12 & -6l & 12 & -6l \\ 6l & 2l^2 & -6l & 4l^2 \end{bmatrix} + \frac{\rho AU^2}{30l}\begin{bmatrix} 36 & 3 & -36 & 3 \\ 3 & 4 & -3 & -1 \\ -36 & -3 & 36 & -3 \\ 3 & -1 & -3 & 4 \end{bmatrix}\right\}\begin{bmatrix} W_1 \\ \theta_1 \\ W_2 \\ \theta_2 \end{bmatrix} = \begin{bmatrix} 0 \\ 0 \\ 0 \\ 0 \end{bmatrix}$$

This is the matrix equation of motion for a single element of the pipe.
It is a second order ordinary differential equation of the form

$$[M]^e\{\ddot{W}\} + [C]^e\{\dot{W}\} + \{[K_s]^e + [K_f]^e\}\{W\} = \{0\} \qquad (15)$$

Where

$[M]^e$ is the Mass matrix.
$[C]^e$ is the Coriolis force matrix.
$[K_s]^e$ is the Pipe Stiffness matrix.
$[K_f]^e$ is the Centrifugal Force matrix

The matrices of Mass or Inertia, Coriolis force, Pipe Stiffness, and Centrifugal force, are respectively given by:

$$[M]^e = \frac{(\rho A + m)l}{420}\begin{bmatrix} 156 & 22l & 54 & -13l \\ 22l & 4l^2 & 13l & -3l^2 \\ 54 & 13l & 156 & -22l \\ -13l & -3l^2 & -22l & 4l^2 \end{bmatrix} \qquad (16)$$

Mass or Inertia Matrix

$$[C]^e = \frac{\rho AU}{30}\begin{bmatrix} -30 & 6 & 30 & -6 \\ 6 & 0 & 6 & -1 \\ -30 & -6 & 30 & 6 \\ 6 & 1 & -6 & 0 \end{bmatrix} \qquad (17)$$

Coriolis Force Matrix

$$[K_s]^e = \frac{EI}{l^3}\begin{bmatrix} 12 & 6l & -12 & 6l \\ 6l & 4l^2 & -6l & -2l^2 \\ -12 & -6l & 12 & -6l \\ 6l & 2l^2 & -6l & 4l^2 \end{bmatrix} \tag{18}$$

Stiffness matrix

$$[K_f]^e = \frac{\rho A U^2}{30l}\begin{bmatrix} 36 & 3 & -36 & 3 \\ 3 & 4 & -3 & -1 \\ -36 & -3 & 36 & -3 \\ 3 & -1 & -3 & 4 \end{bmatrix} \tag{19}$$

Centrifugal Force matrix

2.1.5 Assembly of the Elements Matrices (Assembly Process)
First the zero assembly matrix, a matrix of zeros for all degrees of freedom is written as follows;

$$\begin{bmatrix} 0 & 0 & 0 & 0 & 0 & 0 \\ 0 & 0 & 0 & 0 & 0 & 0 \\ 0 & 0 & 0 & 0 & 0 & 0 \\ 0 & 0 & 0 & 0 & 0 & 0 \\ 0 & 0 & 0 & 0 & 0 & 0 \\ 0 & 0 & 0 & 0 & 0 & 0 \end{bmatrix}$$

Assembling $[K_s]^1$ and $[K_s]^2$ into the zero assembly matrix

$$K_s = \frac{EI}{l^3}\begin{bmatrix} 12 & 6l & -12 & 6l & 0 & 0 \\ 6l & 4l^2 & -6l & 2l^2 & 0 & 0 \\ -12 & -6l & 12+12 & -6l+6l & -12 & 6l \\ 6l & 2l^2 & -6l+6l & 4l^2+4l^2 & -6l & 2l^2 \\ 0 & 0 & -12 & -6l & 12 & -6l \\ 0 & 0 & 6l & 2l^2 & -6l & 4l^2 \end{bmatrix}$$

In a similar way, assembled matrices are obtained from the assembly of the matrices of the centrifugal force term, coriolis force (damping) term and mass (inertia) term respectively:

$$K_f = \frac{\rho A U^2}{30l}\begin{bmatrix} 36 & 3 & -36 & 3 & 0 & 0 \\ 3 & 4 & -3 & -1 & 0 & 0 \\ -36 & -3 & 72 & 0 & -36 & 3 \\ 3 & -1 & 0 & 8 & -3 & -1 \\ 0 & 0 & -36 & -3 & 36 & -3 \\ 0 & 0 & -3 & -1 & -3 & 4 \end{bmatrix}$$

$$C = \frac{\rho A U}{30l}\begin{bmatrix} -30 & 6 & 30 & -6 & 0 & 0 \\ 6 & 0 & 6 & -1 & 0 & 0 \\ -30 & -6 & 0 & 12 & 30 & -6 \\ 6 & -1 & 0 & 0 & 6 & -1 \\ 0 & 0 & -30 & -6 & 30 & 6 \\ 0 & 0 & 6 & 1 & -6 & 0 \end{bmatrix}$$

$$M = \frac{\rho A + m}{420}\begin{bmatrix} 12 & 6l & -12 & 6l & 0 & 0 \\ 6l & 4l^2 & -6l & 2l^2 & 0 & 0 \\ -12 & -6l & 24 & 0 & -12 & 6l \\ 6l & 2l^2 & 0 & 8l^2 & -6l & 2l^2 \\ 0 & 0 & -12 & -6l & 12 & -6l \\ 0 & 0 & 6l & 2l^2 & -6l & 4l^2 \end{bmatrix}$$

2.1.6 Imposition of the boundary conditions

Applying Pinned-Pinned Boundary Condition

at $\quad x = 0 \quad : \quad W = 0 \& \frac{\partial^2 W}{\partial x} = 0$;   (20)

at $\quad x = 0 \quad : \quad W = 0 \quad \& \frac{\partial^2 W}{\partial x} = 0$;   (21)

So that after applying the boundary conditions we have the matrix reduced equation

$$\frac{\rho A + m}{420}\begin{bmatrix} 4l^2 & 13l & -3l^2 & 0 \\ 13l & 312 & 0 & -13l \\ -3l^2 & 0 & 8l^2 & -3l^2 \\ 0 & -13l & -3l^2 & 4l^2 \end{bmatrix}\begin{Bmatrix} \ddot{\theta}_1 \\ \ddot{W}_2 \\ \ddot{\theta}_2 \\ \ddot{\theta}_3 \end{Bmatrix} + \frac{\rho A U}{30}\begin{bmatrix} 0 & 6 & -1 & 0 \\ -6 & 0 & 12 & -6 \\ 1 & 0 & 0 & -1 \\ 0 & 6 & 1 & 0 \end{bmatrix}\begin{Bmatrix} \dot{\theta}_1 \\ \dot{W}_2 \\ \dot{\theta}_2 \\ \dot{\theta}_3 \end{Bmatrix} + \frac{EI}{l^3}\begin{bmatrix} 4l^2 & -6l & 2l^2 & 0 \\ -6l & 24 & 0 & -6l \\ 2l^2 & 0 & 8l^2 & 2l^2 \\ 0 & 6l & 2l^2 & 4l^2 \end{bmatrix}\begin{Bmatrix} \theta_1 \\ W_2 \\ \theta_2 \\ \theta_3 \end{Bmatrix} +$$

$$\frac{\rho A U^2}{30l}\begin{bmatrix} 4 & -3 & -1 & 0 \\ -3 & 72 & 0 & 3 \\ -1 & 0 & 8 & -1 \\ 0 & 3 & -1 & 4 \end{bmatrix}\begin{Bmatrix} \theta_1 \\ W_2 \\ \theta_2 \\ \theta_3 \end{Bmatrix} = \begin{Bmatrix} M_1 \\ F_2 \\ M_2 \\ M_3 \end{Bmatrix} = \begin{Bmatrix} 0 \\ 0 \\ 0 \\ 0 \end{Bmatrix} \qquad (22)$$

2.1.7 Solution of Equation
The equation of motion, equation (15), in finite element formulation, can be written according to Meitrovich (1980) as

$$[M]^e\{\ddot{W}\} + [C]^e\{\dot{W}\} + \{[K_{total}]\}\{W\} = \{0\} \qquad (23)$$

Where

$$[K_{total}] = [K_s]^e - [K_f]^e$$

$[K_{total}]$ is an inconsistent matrix because the two matrices contained in it $[K_s]^e$ and $[K_f]^e$ produce contrary component effects because $[K_f]^e$ acts to weaken the overall stiffness of the pipe. Also, given that the above equation (23) has a gyroscopic damping phrase with an attribute of skew symmetry, $\{/C^T/=/-C/=(-1)^n/C/\}$(for an n × n matrix), the eigenvalue problem can be solved according to the characteristic $[\Omega]$ equivalent to Meitrovich (1980), which is

$$[\Omega] = \begin{bmatrix} -[m + \rho A]^{-1}[C] & -[m + \rho A]^{-1}[K_{total}] \\ [I] & [0] \end{bmatrix} \qquad (24)$$

The results of the eigen value problem yield complex roots. The fundamental natural frequency of the system is described by the imaginary part of the roots while the real part indicates the rate of decay (Mohammed et al., 2016). This solution is implemented in the post processing of the finite element model done with MATLAB.

3.0 Results and Discussions
In the post processing, the following pipe and fluid parameters were defined: pipe length, pipe density, elastic modulus of the pipe, fluid density, pipe internal diameter, fluid flow velocity and number of finite elements. This allowed more freedom for the study to evaluate the relationship between the fundamental frequency of vibration and fluid velocity for pipes of various pipe span lengths and pipe bore diameters, each of which terminated at the point where the critical velocity was reached.

In each case, the fundamental frequency at U=0 is obtained as the natural frequency of the system, and the velocity at which the fundamental frequency ω=0, is obtained as the critical velocity of the system. With respect to this information, the values of critical velocity which is the data of utmost interest in this thesis were collected at each of these pipe span lengths and bore diameters, so that results and graphs are obtained showing the collective profile of the critical velocity as the pipe span length and pipe bore diameters were increased.

The analysis was carried out on the following span lengths of pipe: 2m, 3m, 4m, 5m, and 6m which were discretized into 20, 24, 30, 42, and 50 elements respectively and on 2m pipes of the following bore diameters: 0.0389m, 0.057m, 0.0697m, 0.0856m, 0.111m respectively discretized into 20 elements each. Figure (3) displays fundamental frequency versus fluid velocity plots of the 2m, 3m, 4m, 5m, and 6m pipe span lengths, while figure (4) displays the plot of fundamental frequency against fluid velocity for the 0.0389m, 0.057m, 0.0697m, 0.0856m, 0.111m pipe bore diameters respectively.
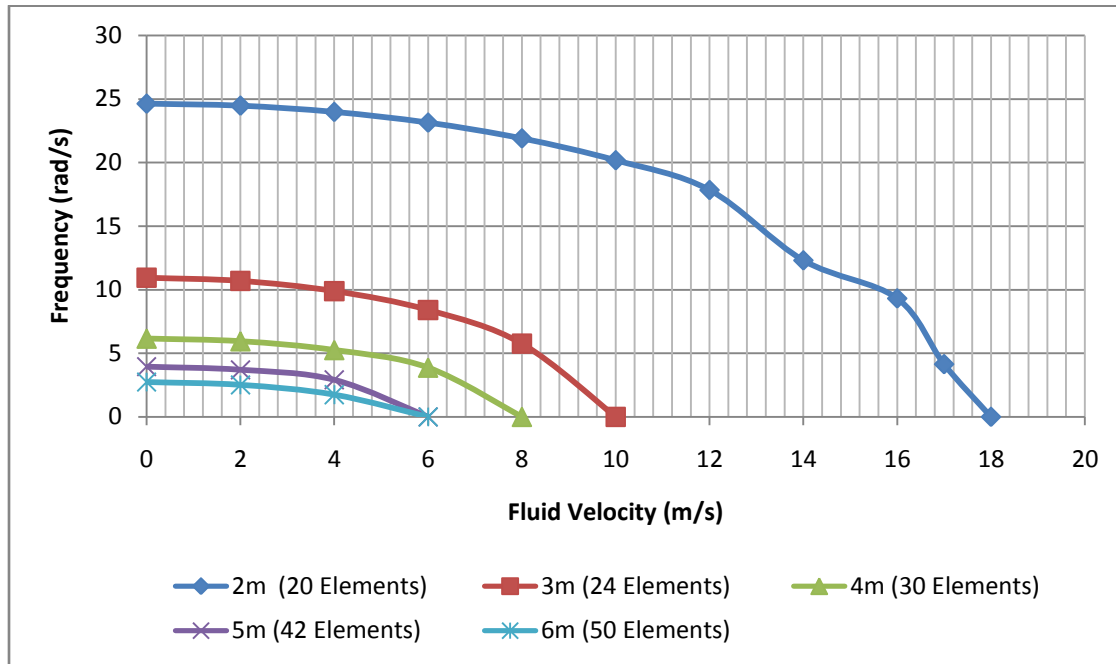
Figure 3: Plots of fundamental frequency against fluid velocity for the pipe span lengths

Figure (3) shows a consistent reduction in the value of critical velocity with increasing pipe span length from 17.8 m/s for a 2m pipe span length to 5.90m/s for a 6m pipe span length. In this case the slenderness ratio of the pipe generally increases with the increasing lengths at a constant diameter; the apparent consequence is that the bending resistance offered by the pipe due to its flexural rigidity against fluid momentum forces is slightly inhibited. Hence, the critical velocity is reached at lower velocities with increasing length. Notice also that the number of discretized elements increased with increased pipe span lengths, this is because the longer pipes required more discrete elements for the finite element solution to converge.
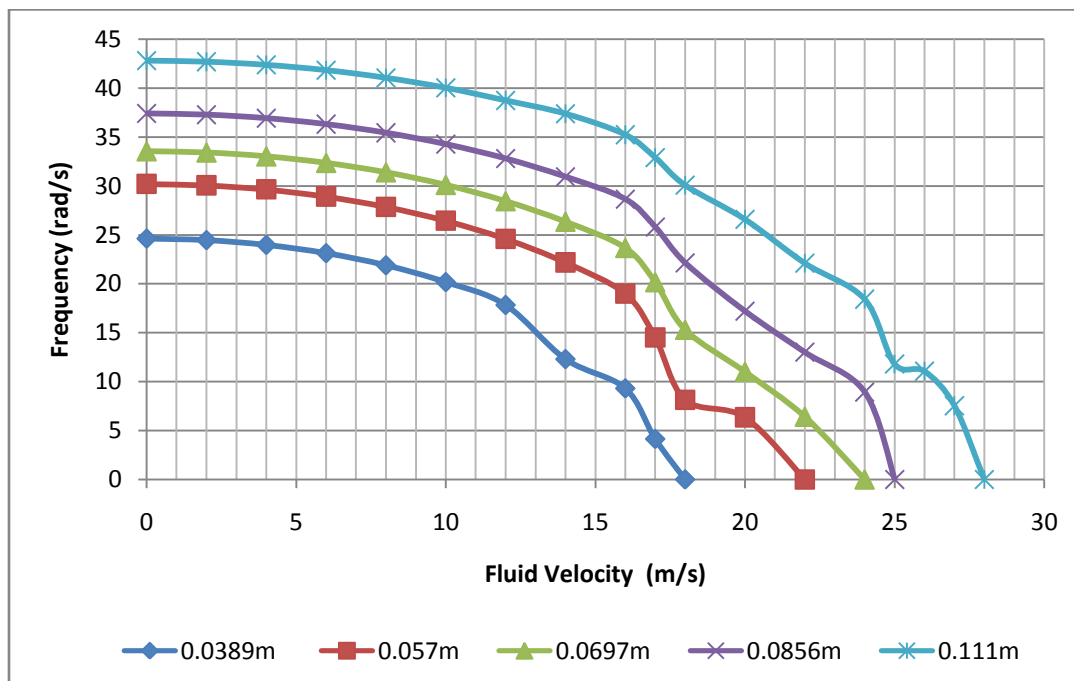

Figure 4: Plots of fundamental frequency against fluid velocity for the pipe bore diameters

Figure (4) on the other hand shows an overall increase in critical velocity with increasing pipe bore diameter from 18m/s at a bore diameter of 0.0389m to 28m/s at a bore diameter of 0.111m. In this case there is a slight reduction in the slenderness ratio of the pipe, an increase in the mass per unit length of the pipe and of the fluid, and then an overall increase in the mass ratio of the system, offering significant resistance to fluid momentum forces producing vibration. Therefore higher velocities are required with increasing pipe bore diameters to reach the zero fundamental frequency where the critical velocity is attained.

In general, both figures (3) and (4) show a consistent reduction in fundamental frequency from the natural frequency at zero fluid velocity to the critical velocity at a fundamental frequency of 0 rad/s. This is due to the fact that at zero fluid velocity, the pipe vibrates strictly under its own weight, depending solely on its mass and stiffness (Jweeg & Ntayeesh 2016) without the influence of the lateral momentum of the fluid, which is fluid velocity dependent, and takes effect as soon as the fluid in the pipe gains velocity up until the critical point of instability at the critical flow velocity.

4.0. Conclusion
From the results of the analysis of internal flow induced vibration of a pinned-pinned pipe carried out using the Finite Element Method; the following conclusions can be drawn:
1. There is a steady reduction in the fundamental frequency of the pipe with increase in flow velocity up to the critical velocity where the fundamental frequency eventually drops to zero.
2. Increasing the pipe span length reduces the critical velocity; therefore, longer pipe-spans have a lower range of stability, in terms of flow velocity, than the shorter pipes of the same bore diameter.
3. Increasing the pipe bore diameter raises the critical velocity value, therefore, for the same pipe span length; pipes with larger bore diameters have a higher stability range in terms of fluid flow velocity.
4. The slenderness ratio of the pipe affects critical flow velocity. The higher the slenderness ratio, the lower the critical velocity. Conversely, lower the slenderness ratio together with an increased mass ratio yields a higher critical flow velocity.

5.0 Recommendation
In this paper, the effect on critical velocity has been studied and analysed for changes in pipe specification while considering internal flow within the pipe. For a more comprehensive grasp of the subject, further studies should be carried out in the following areas:

1. Effect of roughness of pipe walls on the critical flow velocity in the pipe.
2. Effect of fluid/pipe temperature on the critical flow velocity of a pipe in thermal applications.
3. Vibration control system modelling of a fluid conveying pipe.

Nomenclature
L	=	Length of the pipe (m)
S	=	Internal perimeter of the pipe cross section (m)
A	=	Cross sectional area of the pipe (m^2)
F	=	Pressure force per unit length of the pipe (N/m)
ρ	=	Density of the fluid (kg/m^3)
M	=	Mass of the fluid per unit length (kg/m)
m	=	Mass of pipe per unit length (kg/m)
P	=	Fluid applied pressure (kg/m^2)
$Y(x,t) =$		$W(x,t) = W$ = lateral displacement of pipe
Q	=	Transverse shear force (N)
T	=	Longitudinal tension (N)
M	=	Bending moment in the pipe (Nm)
E	=	Young's Modulus (GPa)
I	=	Area moment of inertia
U	=	Fluid Velocity (m/s)
ω	=	frequency of vibration (rad/s)
N_i	=	Shape function of element at node i
N	=	Shape function

$\vec{\mathbf{W}}$	=	the displacement vector
$\vec{\mathbf{W}}^{e}$	=	vector of nodal displacement of an element
$[M]^{e}$	=	Elemental Mass matrix.
$[C]^{e}$	=	Elemental Coriolis force matrix.
$[K_s]^{e}$	=	Elemental Pipe Stiffness matrix.
$[K_f]^{e}$	=	Elemental Centrifugal Force matrix
W_i	=	Nodal displacement/lateral displacement at node i
$\mathbf{F}$	=	Nodal Force
$\boldsymbol{M}$	=	Nodal Moment

References

Ali, H., Al- Hilli&Ntayeesh, T.J. (2013). Free vibration characteristics of elastically supported pipe conveying fluid, *Nahrain University College Of Engineering Journal (NUCEJ), vol.16*

Chellapilla, K. R., Shankarachar, S. &Radhakrishna, M. (2016). Effect of weld tension on flexural frequencies of guided-simply supported fluid conveying pipes. *International Journal of Mechanical Engineering and Automation, 3(8)* pp. 319-324.

Dagh, B.Y. &Sinir,B.G. (2015). Dynamics of transversely vibrating pipes under non-classical boundary conditions. *Universal Journal of mechanical engineering, vol. 3.*

Durrani, N. J. (2001). *Dynamics of pipelines with a finite element method* (Masters Thesis). University of Calgary, Alberta.

Grant, I. (2010). *Flow induced vibrations in pipes, a finite element approach*(Masters Thesis,Cleveland State University, Ohio, United States of America). Retrieved from: http://etd.ohiolink.edu/!etd

Jweeg, M.J. &Ntayeesh, T.J. (2016). Determination of critical buckling velocities of pipes conveying fluid rested on different support conditions. *International Journal of Computer Applications, 134*(10), 34-42. Retrieved from: http://www.ijcaonline.org/archives/volume134/number10/23954-2016908204

Kokare, A.B. &Paward, P.M. (2015).Vibration characteristics of pipe conveying fluid.*Journal of Scientific Engineering and Technology Research, 4(51),* pp (10951-10954).

Meitrovitch , L.,(1980).*Computational methods in structural dynamics*. Sijthoff and Noordhoff International Publisher.

Mohamed, J. A., Mohammed,Q. &Hatem, R. (2016). Stability analysis of pipe conveying fluid stiffened by linear stiffness. *International Journal of Current Engineering and Technology, 6(5)*

Ojetola, A. Jameson, N. J., and Hamidzadeh H.R. (2011). Flow induced vibration and critical velocities. Proceedings of the ASME 2011 International Design Engineering Technical Conference IDETC/CIE.

Paidoussis, M.P., Semler, C. & Lopes, J.L. (2002).Linear and nonlinear dynamics of cantilevered cylinders in axial flow.*Journal of fluids and structures, 16(6)*, pp. 715-737.

Ubani N.O., Dara J. E., Okonkwo U. C., Nwankwojike, B. N. Iheakaghichi C. (2013) Water pipeline network analysis using simultaneous loop flow correction method.*West African Journal of Industrial and Academic Research* 6(1): 4 – 22.

Wen, L., Gonguin, L. &Hoaran, W. (2016).*Dynamic analysis of pipes conveying fluid by transfer matrix method.*Paper presented at the 23[rd]International Conference on Sound and Vibration, Athens, Greece.

Xu, M .R.,Xu, S.P., &Guo, H.Y. (2010). Determination of natural frequencies of fluid-conveying pipes using homotopy perturbation method.*Computers & Mathematics with Applications* 60, 520–52